International Journal of Pharmaceutics 367 (2009) 115–126

Contents lists available at ScienceDirect

International Journal of Pharmaceutics

journal homepage: www.elsevier.com/locate/ijpharm

Molecular interactions in reverse hexagonal mesophase in the presence of Cyclosporin A

Dima Libster[a,1], Paul Ben Ishai[b], Abraham Aserin[a], Gil Shoham[c], Nissim Garti[a,*]

[a] Casali Institute of Applied Chemistry, The Institute of Chemistry, The Hebrew University of Jerusalem, Jerusalem 91904, Israel
[b] Department of Applied Physics, The Hebrew University of Jerusalem, Givat Ram, Jerusalem 91904, Israel
[c] Department of Inorganic Chemistry and the Laboratory for Structural Chemistry and Biology, The Hebrew University of Jerusalem, Jerusalem 91904, Israel

ARTICLE INFO

Article history:
Received 25 June 2008
Received in revised form
18 September 2008
Accepted 22 September 2008
Available online 9 October 2008

Keywords:
Liquid crystals
Reverse hexagonal phase
Glycerol monooleate
Phosphatidylcholine
Cyclosporin A
ATR-FTIR

ABSTRACT

The present work investigates the detailed molecular structure of the H_{II} mesophase of GMO/tricaprylin/phosphatidylcholine/water system in the presence of hydrophobic model peptide Cyclosporin A (CSA) via ATR-FTIR analysis. The conformation of the peptide in the hexagonal mesophase, as well as its location and specific interactions with the components of the carrier, were studied. Incorporation of phosphatidylcholine to the ternary GMO/tricaprylin/water system caused competition for water binding between the hydroxyl groups of GMO and the phosphate groups of the phosphatidylcholine (PC) leading to dehydration of the GMO hydroxyls in favor of phospholipid hydration. Analysis of CSA solubilization effect on the H_{II} mesophase revealed a significant increase in the strength of hydrogen bonding with surfactant hydrogen-bonded carbonyls, indicating interaction of the peptide with the C=O groups of the surfactants. The peptide probably caused partial replacement of the intramolecular hydrogen bonds of the mesophase carbonyl groups with intermolecular hydrogen bonds of these carbonyl groups with the peptide. Furthermore, analysis of the Amide I' peak in the FTIR spectra of the peptide demonstrated that two pairs of its internal hydrogen bonds are disrupted when it is incorporated. The partial disruption of the internal hydrogen bonds seems to cause an outward rotation of the peptide amide groups involved, resulting in more efficient intermolecular hydrogen-bonding ability. Apparently, this conformational change increased the hydrophilic properties of CSA, even making it susceptible to a weak interaction with the GMO hydroxyl groups in the interfacial region.

1. Introduction

Polar lipids are an important group of biocompatible amphiphiles, with applications in several fields, such as food systems (Sagalowicz et al., 2006a), the synthesis of template-ordered materials (Bender et al., 2007; Dan-Dan et al., 2008) and various pharmaceutical applications (Drummond and Fong, 1999; Clogston and Caffrey, 2005; Shah and Paradkar, 2005; Farkas et al., 2007; Efrat et al., 2008). Lipids and nonionic surfactants exhibit rich phase behavior depending on the composition of the physicochemical conditions. The most common lyotropic liquid crystalline phases are lamellar (L_α), hexagonal (normal, [H_1] or inverted [H_{II}]) and normal or inverted cubic (bicontinuous or micellar) structures (Larsson, 1989; Qiu and Caffrey, 2000).

Reverse hexagonal lyotropic liquid crystals (H_{II}) seem to be promising candidates as alternative delivery vehicles for pharmaceuticals due to their special structural properties. These structures can accommodate biologically active molecules either within the aqueous domains, composed of dense packed, infinitely long and straight water-filled rods, or by direct interaction within the lipid hydrophobic moieties, orientated radially outward from the centers of the water rods (Fig. 1) (Amar-Yuli et al., 2007a; Libster et al., 2008). Due to these properties, H_{II} mesophases can be specifically used to solubilize and transport therapeutic peptides and proteins by both oral and transdermal routes. Moreover, these liquid crystalline phases retain its internal structure, morphology and stability upon high water concentration (~95 wt%), which correspond to oral delivery conditions (Amar-Yuli et al., 2007a). When delivered as is, without a protecting carrier, biomacromolecules are susceptible to cleavage by a large array of human proteases and they, therefore, usually display poor bioavailability (Gabizon et al., 2003; Getie et al., 2005). The practical application and the specific solubility potential of poorly water soluble drugs and their release from H_{II} mesophases was recently demonstrated *in vitro* and *in vivo* for several such biomolecules, including vitamin K (Lopes et al., 2007),

* Corresponding author. Tel.: +972 2 658 6574/5; fax: +972 2 652 0262.
E-mail address: garti@vms.huji.ac.il (N. Garti).

[1] The results presented in this manuscript will appear in the Ph.D. dissertation of D.L. in partial fulfillment of the requirements for the degree of Doctor in Applied Chemistry, The Hebrew University of Jerusalem, Israel.

0378-5173/$ – see front matter © 2008 Elsevier B.V. All rights reserved.
doi:10.1016/j.ijpharm.2008.09.048

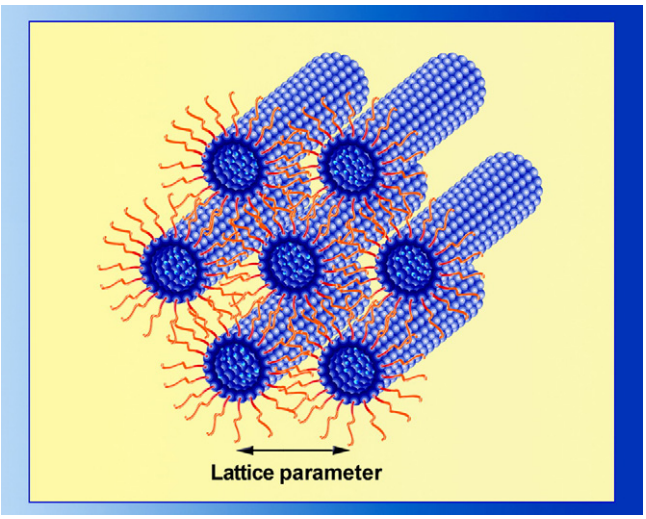

Fig. 1. Schematic presentation of H_{II} mesophase, illustrating the packing of infinitely long water-filled rods, surrounded by lipid layers.

cinnarizine (Boyd et al., 2007), paclitaxel and irinotecan (Boyd et al., 2006), progesterone (Swarnakar et al., 2007) and cyclosporin A (Lopes et al., 2006a,b).

Cyclosporin A (CSA) (Fig. 2) is a highly lipophilic, 11 amino acid cyclic peptide, recognized as one of the most effective immunosuppressive agents used for transplantation medicine and dermatology (Aliabadi et al., 2007; Woo et al., 2007; Zidan et al., 2007; Song et al., 2008). Nevertheless, oral administration of this cyclic peptide is limited by its low bioavailability (Gursoy and Benita, 2004). Although several dedicated delivery systems for CSA have been developed, their overall performance and efficacy are yet to be improved. In particular, there is still a specific requirement for controlled release systems to maintain the blood levels of the drug within the therapeutic range for significantly longer durations than are possible at present (Italia et al., 2006; Liu et al., 2007). The immunosuppressive effect, as well as the side effects of CSA, is thought to be influenced by the partitioning of the molecule into the membrane bilayer (Legrue et al., 1983; Lambros and Rahman, 2004).

A number of studies aimed to explore the binding and release of CSA to liposomal membranes and the pharmacokinetic impact of such processes (Fahr and Seelig, 2001; Fahr et al., 2005). As a highly lipophilic drug, CSA is expected to be intercalated deeply into the hydrophobic core of the carrier. In this case there should be a considerable energetic barrier for CSA to partition into the water phase, at least from the thermodynamic point of view. Surprisingly, however, these predictions do not correlate with the experimentally monitored kinetics of the transfer process. Despite its high

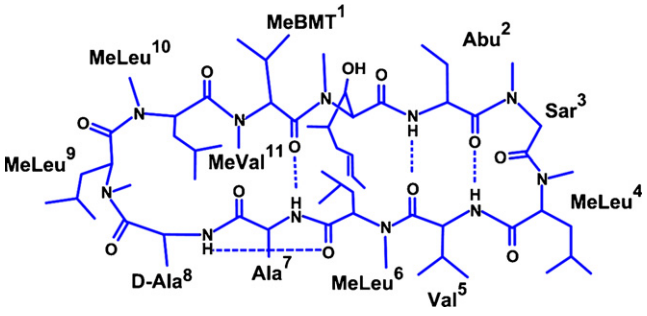

Fig. 2. Chemical structure of Cyclosporin A (Zijlstra et al., 2007).

lipophilicity, CSA was found to exhibit remarkably high exchange rates between liposomes (Fahr and Seelig, 2001). Simply taken, such observations may indicate that, although unexpected, CSA molecules can migrate out of the lipophilic layer of a liposome, dynamically cross aqueous media and integrate in the lipophilic layer of another liposome. This surprising behavior of CSA has not been explained on the molecular or structural level, as yet. Along the same line, Lopes et al. (2006a) demonstrated increased CSA skin penetration from both cubic and reverse hexagonal liquid crystalline phases of GMO/water and GMO/water/oleic acid, respectively. To account for these observations, general interactions were assumed between the polar groups of the peptide and monoolein in the cubic phase.

Solubilization of CSA within the reverse hexagonal phase has been further studied in our laboratory. In previous reports we described a GMO/water system with solubilized tricaprylin displaying a reverse hexagonal phase at room temperature over a relatively broad range of compositions (Amar-Yuli and Garti, 2005). In addition, it was found that phosphatidylcholine (PC) can be incorporated into the ternary GMO/tricaprylin/water hexagonal system (Libster et al., 2007). Solubilization of PC improved the elastic properties of the H_{II} mesophase and enhanced its thermal stability. In those studies we demonstrated that CSA was solubilized into the H_{II} mesophases, and its phenomenological solubilization effects were studied on a macroscopic scale (Libster et al., 2007). It is clear, however, that a detailed molecular characterization of the interactions between CSA and the H_{II} mesophase is required in order to understand and improve such a solubilization system for controlled delivery and release applications.

The present report describes a series of studies that focused on the detailed structural behavior of H_{II} mesophases with and without solubilized guest molecules. We especially concentrated on the molecular structure of the quaternary system composed of GMO/tricaprylin/phosphatidylcholine/water, which was studied mainly via ATR-FTIR spectroscopic analysis.

ATR-FTIR is a well-established experimental technique that is particularly powerful for probing the molecular structure of liquid crystals (Holmgren et al., 1988; Nilsson et al., 1994; Talaikytė et al., 2004; Misiunas et al., 2005; Amar-Yuli et al., 2007b, 2008). It was also shown to be a good tool to characterize the secondary structure of peptides and proteins (Dong et al., 1990; Vass et al., 2003; Barth, 2007). Consequently, it was employed to study the structure and conformation of the peptide drug CSA, its structural changes during solubilization in the hexagonal mesophase, and its location and specific interactions with the various components of the mesophase.

2. Materials and methods

2.1. Materials

Monoolein, GMO, distilled glycerol monooleate (min. 97 wt% monoglyceride), 2.5 wt% diglyceride and 0.4 wt% free glycerol (acid value 1.2, iodine value 68.0, melting point 37.5 °C) were obtained from Riken Vitamin Co. (Tokyo, Japan). Tricaprylin (TAG) (97–98 wt%) was purchased from Sigma Chemical Co. (St. Louis, MO). Phosphatidylcholine of soybean origin (Epikuron 200, min. 92% PC) was obtained from Degussa BioActives GmbH. (Hamburg, Germany). Cyclosporin A was purchased from LC Laboratories (Woburn, MA, USA). The water was double distilled. All ingredients were used without further purification. D_2O (D, 99.9%) was purchased from Cambridge Isotope Laboratories Inc. (Andover, MA, USA).

2.2. Preparation of H_{II} mesophases

The starting composition of 72 wt% GMO and 8 wt% tricaprylin (9:1 weight ratio) at water content of 20 wt% was chosen for the solubilization experiments. In order to study the influence of PC on the mesophases it was solubilized at 5–18 wt% concentrations, decreasing the GMO and tricaprylin concentrations but keeping their weight ratio of GMO/tricaprylin (9:1) and water content of 20 wt% constant. The GMO/PC/tricaprylin/water hexagonal liquid crystals were prepared by mixing weighed quantities of GMO, tricaprylin, and PC while heating to 80 °C. This was done in sealed tubes under nitrogen atmosphere to avoid oxidation of the GMO and PC. An appropriate quantity of preheated water at the same temperature was added and the samples were stirred and cooled to 25 °C. Cyclosporin A was solubilized in the range of 1–6 wt% using starting composition of 63 wt% GMO and 7 wt% tricaprylin (9:1 weight ratio) and 10 wt% PC at D_2O content of 20 wt%. D_2O was used for FTIR measurements. It should be noted that as a result of CSA solubilization the concentrations of GMO and tricaprylin were decreased, keeping their weight ratio of GMO/tricaprylin (9:1), water content of 20 wt% and PC content of 10 wt% constant. Cyclosporin A was first dissolved in GMO prior to incorporation to GMO/PC/tricaprylin mixtures. The thermal stability of the peptide was verified by FTIR analysis of Amide I band after heating and cooling cycles and DSC analysis (data not shown). CSA is thermally stable up to 120 °C the peptide is thermally stable. At this temperature it undergoes T_g transition (Hussain et al., 2004). The samples were allowed to equilibrate for 24 h before examination.

2.3. Small angle X-ray scattering (SAXS)

Scattering experiments were performed using Ni-filtered Cu Kα radiation (0.154 nm) from an Elliott rotating anode X-ray generator that operated at a power rating of 1.2 kW. The X-ray radiation was further monochromated and collimated by a single Franks mirror and a series of slits and height limiters, and measured by a linear position-sensitive detector. The samples were held in 1.5 mm quartz X-ray capillaries inserted into a copper block sample holder. The temperature was maintained at $T \pm 0.5$ °C with a recirculating water bath. The camera constants were calibrated using anhydrous cholesterol. The scattering patterns were desmeared using the Lake procedure implemented in home-written software (Lake, 1967).

2.4. Attenuated total reflectance Fourier transform infrared (ATR-FTIR) measurements

An Alpha model spectrometer, equipped with a single reflection diamond ATR sampling module, manufactured by Bruker Optik GmbH (Ettlingen, Germany), was used to record the FT-IR spectra. The spectra were recorded with 50 scans, at 25 °C; a spectral resolution of 2 cm^{-1} was obtained.

2.5. ATR-FTIR data analysis

Multi Gaussian fitting has been utilized to resolve individual bands in the spectra. The peaks were analyzed in terms of peak frequencies, width at half-height and areas. In order to resolve the measured Amide I' band of CSA the samples' spectra were background subtracted against the appropriate hexagonal mesophase control spectra. Further, the Amide I' band was resolved by second derivative Savitzky–Golay nine-point smoothing function.

Table 1
Resolved ATR-FTIR bands for GMO/PC/tricaprylin/H_2O system, containing GMO/tricaprylin constant weight ratio of (9:1), 20 wt% H_2O and varied PC concentrations in the range of 0–18 wt%.

Molecule	Band	Wavenumber range (cm^{-1})
Monoglyceride	β–C–OH stretching	1119–1121
	γ–C–OH stretching	1049–1054
PC	Symmetric stretching mode PO_2^-	1089–1086
Tricaprylin	C–O stretching	1111–1104

3. Results and discussion

3.1. The influence of PC on the tenary GMO/tricaprylin/water mixtures

An ATR-FTIR temperature-dependent study conducted recently in our laboratory demonstrated the power of this methodology for the detailed analysis of molecular interactions that take place in the ternary GMO/tricaprylin/water reverse hexagonal mesophase (Amar-Yuli et al., 2007b, 2008). A similar approach was adopted for the present study, in order to clarify the structure and interactions of the peptide drug CSA with a reverse hexagonal mesophase structure.

Prior to studying peptide–mesophase interactions, it is important to obtain the molecular level picture of the interaction governing the structural properties of the mixed nonionic and zwiterionic surfactants (GMO and PC) in these liquid crystals. We especially focused on the structural influence of PC on the ternary GMO/tricaprylin/water mixtures. The structure was investigated in terms of the water–surfactant interface region in the vibrational range of 1000–1200 cm^{-1} (Fig. 3a). The peak assignments of the IR spectra were done according to procedures described in detail in previous reports (Holmgren et al., 1988; Nilsson et al., 1991, 1994; Razumas et al., 1996; Guillén and Cabo, 1997; Amar-Yuli et al., 2007b, 2008). At the interface, several vibrational modes were analyzed by fitting the observed spectra with multiple Gaussians, reflecting the interfacial packing of the lipid headgroups (Fig. 3b). For GMO, two hydroxyls could be identified in the observed spectra: C–OH (β, ∼1117 cm^{-1}), C–OH (γ, ∼1051 cm^{-1}), and C=O (carbonyl at the α position, 1720–1740 cm^{-1}). C–O stretching vibration of tricaprylin was detected at ∼1110 cm^{-1}. The interfacial behavior of PC was followed by the phosphate symmetric stretching mode at ν_S-PO_2^- at 1088 cm^{-1}. As demonstrated previously, the phosphate groups of lipids bind water molecules and the sensitivity of the phosphate vibrations to hydration has been well documented (Hübner and Blume, 1998). It was found that the asymmetric PO_2^- vibrational band (1250–1230 cm^{-1}) is extremely sensitive to hydration; however, this band was overlapped with the tricaprylin C–O and CH_2 bands and could not be reliably resolved. Upon increasing the PC concentration in the mesophases, the phosphate symmetric stretching mode of ν_S-PO_2^- at 1088 cm^{-1} could be observed. In a similar way, it was previously found that the symmetric stretching mode of ν_S-PO_2^- was also sensitive to hydrogen-bonding modifications (Hübner and Blume, 1998). Table 1 summarizes the mentioned resolved band for this system.

Analysis of the data presented in Fig. 3a revealed that a gradual linear transition toward higher wavenumbers from 1049 to 1054 cm^{-1} was obtained at the γ–C–OH band (Fig. 4a). As expected, the stronger the hydrogen bonding between the functional groups, the lower the stretching frequency. The frequency shift suggests a conformational change of the γ–C–OH group that occurred as a result of decreasing interaction in the surroundings of the vibrational entity, probably a decrease in hydrogen bonding. Since the water concentration was kept constant during all experiments, a

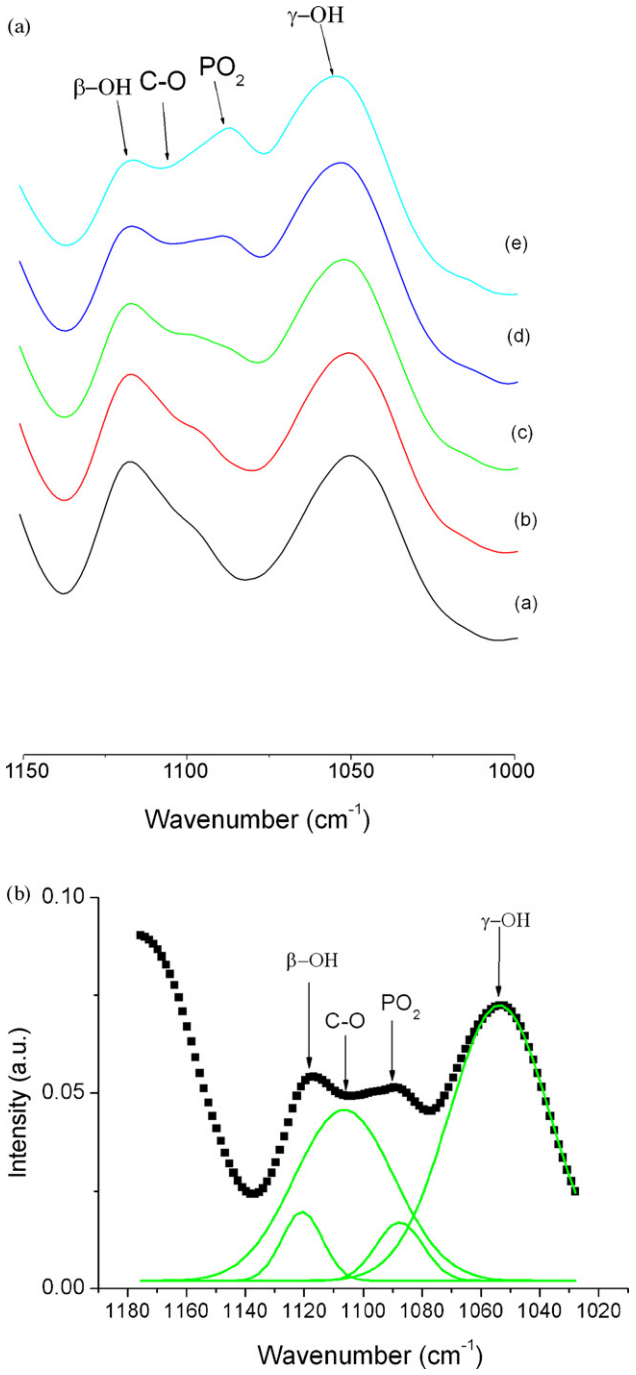

Fig. 3. (a) ATR-FTIR spectra of the H_{II} mesophases of GMO/PC/tricaprylin/water systems with concentration containing (a) 0 wt% PC, (b) 5 wt% PC, (c) 8 wt% PC, (d) 13 wt% PC, (e) 18 wt% PC. Four absorption bands are shown: β and γ hydroxyls for GMO, symmetric stretching mode of ν_S-PO_2^- for PC and C–O for tricaprylin. (b) Representative ATR-FTIR data fitting with four gaussians of the H_{II} mesophases of GMO/PC/tricaprylin/water system containing 18 wt% PC.

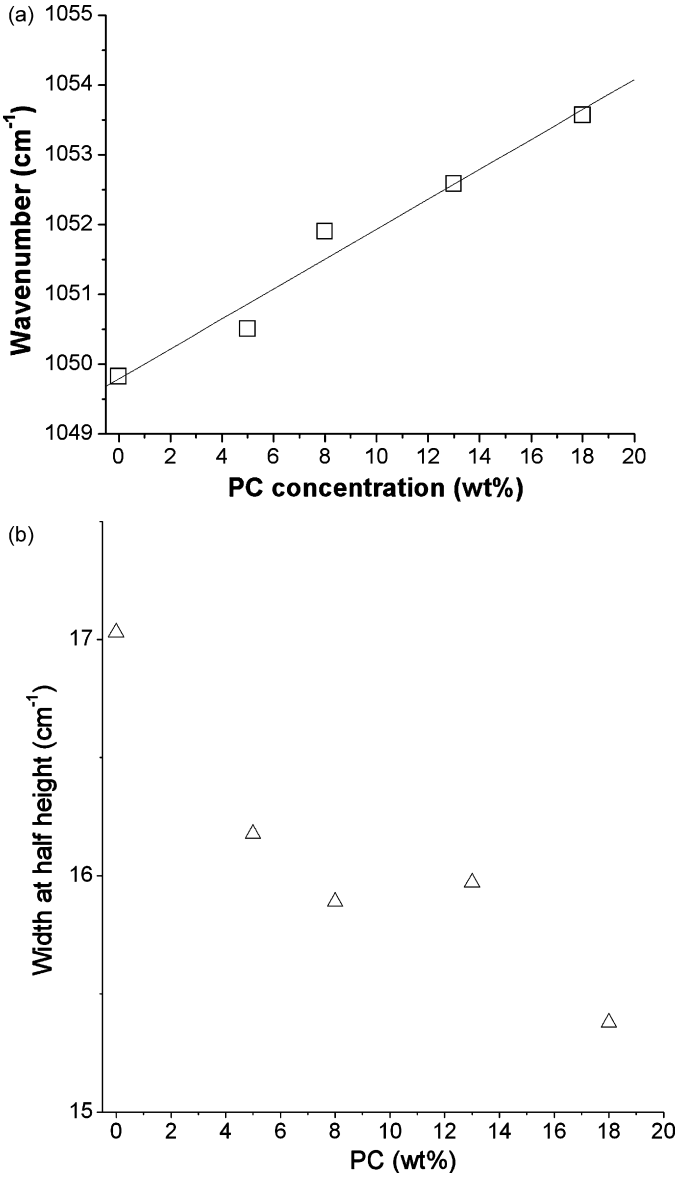

Fig. 4. (a) Frequency (cm^{-1}) as a function of PC concentration (wt%) of the γ–C–OH absorption mode of GMO molecule. (b) Width at half-height (cm^{-1}) as a function of PC concentration (wt%) of the γ–C–OH absorption mode.

competition for water binding takes place between the γ–C–OH groups of GMO and the phosphate groups of the PC. This led to hydration of the phosphate groups at the expense of partial dehydration of the γ–C–OH groups. From the structural point of view this increase in frequency may be also explained through the decreasing curvature of the mesophases and lower degree of packing at the interface as a result of an increase in the lattice parameter of the structures (5 Å) (Libster et al., 2007), as caused by the solubilization of PC. Simultaneously, the intensity of the symmetric stretching mode of the ν_S-PO_2^- band gradually increased due to the phospholipid concentration increase, since it is proportional to the concentration of the absorbing species, as shown in Fig. 3a. At the same time, a slight shift of the ν_S-PO_2^- band to lower wavenumbers was detected from 1089 to 1086 cm^{-1}. This could indicate stronger water binding of the phosphate head group and/or hydrogen bonding with GMO head groups. Nilsson et al. (1991) showed that in the L_α and cubic phases of the GMO/water system, the γ–C–OH group forms an intramolecular hydrogen bond to the carbonyl group of GMO, which, by addition of DOPC, is broken and hydrogen bonding between the GMO hydroxyl groups and DOPC phosphate group is formed. Thus, it could also be suggested that a fraction of these intramolecular hydrogen bonds is also broken and replaced by intermolecular hydrogen bonds with the polar PO_2^- groups. Such interaction with phospholipids also significantly altered the conformation of the β–C–OH monolein head group. At the β–C–OH (1117 cm^{-1}) position of GMO a noticeable decrease in peak intensity (up to 40%) was detected (Fig. 3a), accompanied

with narrowing of the band, and a weak frequency shift from 1119 to 1121 cm^{-1}. These findings also suggested moderate dehydration of the β–C–OH groups, which were initially less hydrated, compared with γ–C–OH groups. The significant intensity decrease also indicates that PC moieties are intercalated in the vicinity of the β–C–OH groups, lowering the packing density of these hydroxyls. This is reflected by the decreased number of absorbing molecules at this stretching band. The width at half-height of both the β (data not shown) and γ peaks (Fig. 4b) were reduced as the PC concentration was increased. As less hydration around the OH groups would lead to more uniformity in the weaker C–OH bond and restricted mobility of these groups, it is indeed consistent with the observation in the peak frequencies.

C–O stretching vibration of tricaprylin was detected at ~1111 cm^{-1} in the absence of PC and a total low-frequency shift of this band (7 cm^{-1}) was observed when the concentration of the phospholipid was increased to 18 wt% PC (data not shown). It should be pointed out that, for pure TAG, this CO–O band was found at 1100 cm^{-1}. These observations suggest that PC incorporation into the mesophases caused the CO–O groups of TAG to adopt a conformation that is closer to that of its pure state. According to our previous NMR measurements, at room temperature TAG molecules are located in the interstices within the densely packed cylindrical aggregates of GMO close to the interface region (Amar-Yuli et al., 2007b). According to this kind of interpretation, competition is taking place between the PC and TAG molecules for the solvation of the GMO tails and part of the triglyceride molecules are "salted out" in favor of the PC–GMO interactions, suggesting conformation closer to its pure state.

In one of our previous reports we have shown that bulk properties of the ternary system of GMO/TAG/water were significantly modified by incorporation of PC (Libster et al., 2007). SAXS analysis demonstrated gradual increase in the lattice parameter of the mesophases from 57.1 Å in the system without PC up to 62.5 Å in the presence of 20 wt% PC. The tendency of PC to increase the lattice parameter is correlated to the present results from the ATR-FTIR measurements. Two competing effects are contributed to the described behavior. Hydration of PC is supposed to increase the lattice parameter, while the dehydration of GMO should hinder this process. However, the hydration of the larger size polar moieties of PC is probably more dominating, compared to the partial dehydration of the hydroxyls of GMO, and therefore responsible for the slow and relatively moderate swelling of the structures (up to 5 Å). The presence of PC in the mixture had also a significant effect on the thermal processes in the mesophase. The change was reflected in a decrease of the melting temperature (T_m) of the GMO/tricaprylin thermal transition of almost 3 °C, which was accompanied by a pronounced and progressive enthalpy (ΔH_f) decrease from 37.3 J/g in the system without PC to 2.7 J/g in the mesophase containing 20 wt% PC. In accordance with this kind of interpretation of the FTIR results, it is very likely that the intramolecular hydrogen bonding of GMO molecules is partly broken and the intermolecular hydrogen bonds between the GMO and the PC polar head groups were partly formed. Due to the highly polar nature of phosphate groups, and the competition of these groups with GMO hydroxyl groups for water, the PC and GMO interactions are expected to strengthen the interface and hence influence the rheological properties of the resulting structures. Since the major rheological properties of the LLC depend mostly on the topology of the water–lipid interface (Sagalowicz et al., 2006b) these properties should reflect the expected alterations. One such parameter is the maximum relaxation time (τ_{max}), which is regarded as the time scale for relaxation to the equilibrium configuration of the water–lipid interface. A noticeable increase in τ_{max} was detected with increase in the quantity of added PC, suggesting a more elastic response (Libster et al., 2007).

Table 2
Resolved ATR-FTIR bands for GMO/PC/tricaprylin/D_2O/CSA system containing GMO/tricaprylin constant weight ratio of (9:1), 20 wt% H_2O, 10 wt% PC and varied CSA concentrations in the range of 0–6 wt%.

Molecule	Band	Wavenumber range (cm^{-1})
Monoglyceride	Symmetric CH_2 stretching	2853
	Antisymmetric CH_2 stretching	2918
	"Free" carbonyls C=O stretching	1743
	"Bounded" C=O groups	1727–1722
	CO–O bond (ester) stretchings	1164–1166
		1177–1184
D_2O	O–D stretching	3386–3396
Cyclosporin A (Amide I' band)	Anti-parallel β-sheet with two hydrogen bonds: Ala^7NH to $MeVal^{11}$C=O and D-Ala^8NH to $MeLeu^6$C=O	1624–1625
	H-bonded γ-turn formed with D-Ala^8NH to $MeLeu^6$C=O hydrogen bonding	1632
	Type II β-turn stabilized by two hydrogen bonds – Abu^2NH to Val^5C=O and Val^5NH to Abu^2C=O	1639
	Inverse γ-loop consisting of at D-Ala^8, $MeLeu^9$ and $MeLeu^{10}$	1650
	Type II β-turn located at Sar^3 and $MeLeu^4$	1669–1672
	Intramolecular hydrogen bond between the β-OH on $MeBmt^1$ and the $MeBmt^1$C=O	1679–1681
	"Free", non-hydrogen-bonded C=O of the β-sheet	1690–1700

Hence, it was found that despite the relatively low concentration of the zwiterionic PC (compared to the corresponding concentration of GMO) in the H_{II} mesophases, it has a significant impact on both the microscopic and mesoscopic properties of these liquid crystal structures.

3.2. CSA influence on the H_{II} mesophase

The mutual influence of the peptide on the structure of the GMO/tricaprylin/PC/CSA/D_2O mesophases was elucidated using D_2O instead of H_2O in order to avoid the influence of the water OH bending on the Amide I' band of CSA. The resolved bands, reflecting the influence of CSA on the H_{II} mesophase, are presented in Table 2. Prior to the FTIR measurements, we verified that the structure remained hexagonal when the pure water was replaced by D_2O at the same hydration level (20 wt%). Typical SAXS diffraction pattern of the H_{II} mesophase, containing D_2O is presented in Fig. 5. Slight increase of 2.5 Å in lattice parameter (from 59.2 to 61.7 Å) was monitored when D_2O was used, compared to the H_2O based samples, which is attributed to the more tight bonding of D_2O with the surfactants hydrophilic moieties. Like in the H_2O based samples (Libster et al., 2007) only minor changes (increase) in the lattice parameter in the range of 1 Å was recorded upon CSA solubilization in the concentration up to 6 wt%.

Considering the fact that CSA is a highly hydrophobic molecule, it was originally reasonable to assume that it was mainly incorporated between the acyl chains of the surfactants. We therefore followed the specific IR peaks of GMO methylene groups (Fig. 6) at 2853 cm^{-1} (symmetric stretching) and at ~2918 cm^{-1} (antisymmetric stretching). Generally, it is widely accepted that the absorption at 2853 cm^{-1} is associated with the conformational order of the lipid chain, which reflects the instantaneous state of organization of the membranes (Mendelsohn et al., 1991). This band at 2853 cm^{-1} is also known to be rather sensitive to *trans-gauche* isomerization within the chain (Fournier et al., 2008). Nevertheless, we did not detect any significant changes in the frequency of these bands. Our conclusion is, therefore, that there is

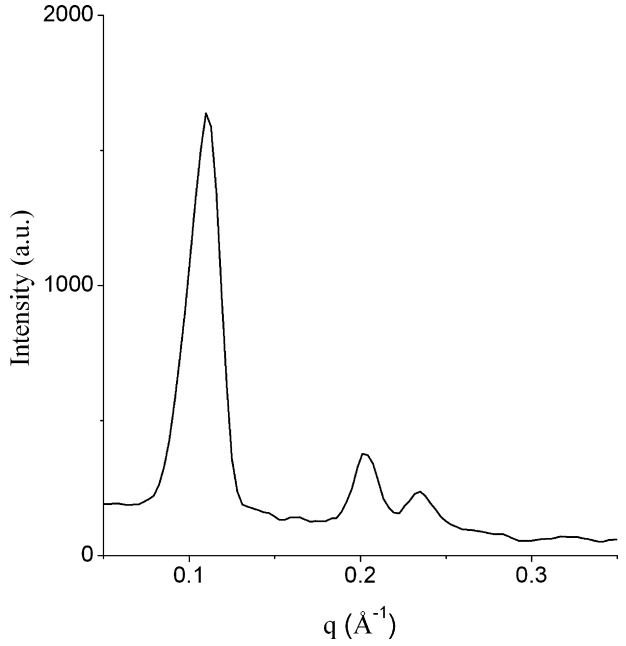

Fig. 5. Small-angle X-ray scattering pattern of GMO/tricaprylin/PC//D_2O mesophase containing GMO:tricaprylin 9:1 wt ratio, 20 wt% D_2O, 10 wt% PC, at 25 °C. The d-spacings of the three Bragg peaks are observed to be related by the ratio of $1 : 1/\sqrt{3} : 1/\sqrt{4}$, consistent with two-dimensional hexagonal symmetry. $d = 2\pi/q$, where q is the amplitude of the scattering vector.

no evidence for an isomerization process in the particular system examined.

Furthermore, CH_2 wagging mode in the IR spectral region of 1330–1400 cm^{-1} was observed (data not shown). It provides information on the effect of the CH_2 groups involved in nonplanar (*gauche*) conformers (Razumas et al., 1996). A close examination of this spectral mode, consisting of the end-gauche band (eg) at ~1341 cm^{-1}, the double gauche band (gg) at ~1354 cm^{-1}, and the band of gauche-*trans*-gauche (kink) at ~1367 cm^{-1}), does not indicate any significant conformational change. However, a noticeable

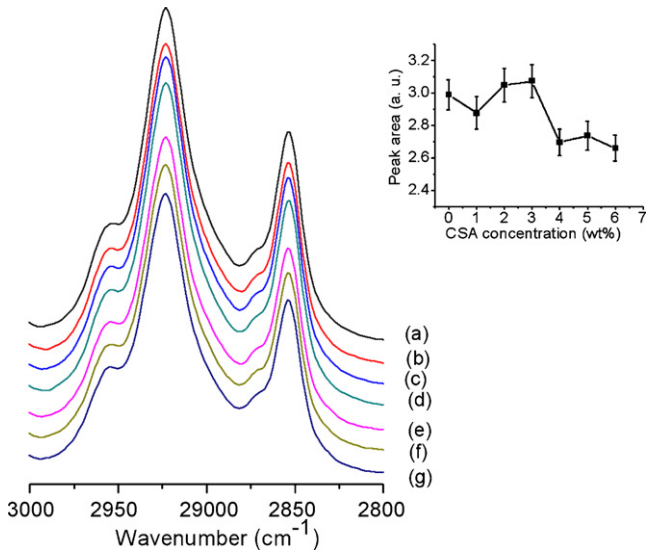

Fig. 6. ATR-FTIR spectra of the H_{II} mesophases of GMO/PC/tricaprylin/water/CSA systems with CSA concentrations of (a) 0% (b) 1%, (c) 2%, (d) 3%, (e) 4%, (f) 5%, (g) 6% in frequency range of 3000–2800 cm^{-1}. The graphs depict the decrease in peak area with increasing CSA concentration with onset of the critical behavior of 4 wt% CSA at the 2853 cm^{-1} absorption band.

decrease in the peak area of the symmetric (Fig. 6) and antisymmetric (data not shown) stretching modes was monitored as a function of the incorporated peptide, starting from a CSA concentration of 4 wt%. Such decrease in the peak area may result from the packing density decrease of the surfactant tails, which is dictated only by the physical embedding of the relatively high concentration of the drug into the hydrocarbon region. With this indication in mind, we further looked for stronger and more direct evidences of the CSA interactions with the mesophase components.

The carbonyl absorption mode was found to be sensitive for protein–surfactant interactions. The carbonyl band exhibits two clearly separated peak maxima (Fig. 7a), suggesting that this group is exposed to two different environments: the first one originates from 'free' carbonyls (1743 cm^{-1}) and the second comes from intramolecularly hydrogen-bonded carbonyl groups (1727 cm^{-1}) (Fig. 7b). It was found that while there was no effect on the free C=O band position, the peak frequencies for the bonded carbonyl groups demonstrate a monotonic decrease from 1727 to 1722 cm^{-1} as CSA concentration is increased (Fig. 8a). This finding shows that the strength of hydrogen bonding was increased as a result of the peptide solubilization, suggesting an interaction of the peptide with the C=O groups. Furthermore, the width at half-height of the lower frequency carbonyl mode was decreased, but the opposite trend was noticed in the width at half-height values of the high frequency band (Fig. 8b). The implication is ordering or more restricted motion of the intramolecularly bound carbonyls and an increased degree of rotation of the free carbonyls as a function of CSA embedment. These conclusions were further reinforced by comparing the peak areas of the free and hydrogen-bonded carbonyls. In order to account for concentration changes as the concentration of CSA was increased, the normalized peak areas ($A_{free}/(A_{free} + A_{bonded})$) and $A_{bonded}/(A_{free} + A_{bonded})$ were calculated (Fig. 9). Here it is clear that the number of hydrogen-bonded carbonyls is reduced in favor of freely rotating groups when the CSA is introduced. Therefore, the solubilization of the peptide probably induced partial replacement of the intramolecularly hydrogen-bonded carbonyl groups bonds to carbonyl–CSA bonds. However, not all the hydrogen bonds that were disrupted by the CSA solubilization were reoccupied by peptide–carbonyl bonds. These results indicate that CSA is partly intercalated in the interfacial region. Considering the fact that SAXS results (Libster et al., 2007) revealed only minor changes in the lattice parameter of the mesophases (increase of 1–1.5 Å), it can be suggested that the intercalation of CSA did not cause significant modifications of the curvature but rather influenced the intramolecularly hydrogen-bonded carbonyl groups.

Following the interfacial behavior of the peptide, the CO–O bond (ester) stretching mode of the surfactants was examined (Fig. 10a). The absorption maximum monitored at ~1176 cm^{-1} was resolved by Gaussian fitting to two peaks (1164 and 1177 cm^{-1}), probably corresponding to different conformations of the ester moieties. The incorporation of CSA gave rise to a gradual shift of the two absorption maxima toward higher wavenumbers with increasing peptide concentration (Fig. 10b). According to Hübner and Mantsch (1991) and Razumas et al. (1996), the low frequency position of the CO–O band can be associated with a deviation from the dihedral angle of 180° in this segment, induced by torsional motions or by a small population of gauche conformers near the sn-1 CO–O single bond. The authors showed that lower frequency positions of the CO–O band correspond to more disordered states of the lipids. Hence, we conclude that solubilization of CSA, which resulted in a higher frequency position of CO–O band, implied a more ordered state of CO–O bond.

Regarding the strong interfacial behavior of the peptide we examined the absorption bands at 3200–3400 cm^{-1}, attributed to the O–H stretching modes (υ_{OH}), which are used to characterize the

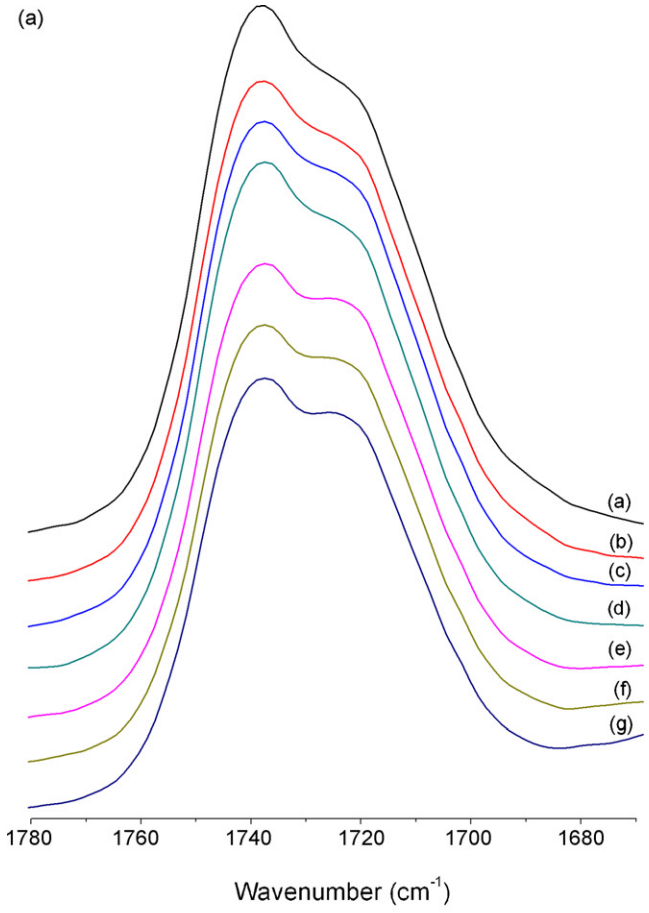

Fig. 7. (a) ATR-FTIR spectra of the H_{II} mesophases of GMO/PC/tricaprylin/water/CSA systems with CSA concentrations of (a) 0%, (b) 1%, (c) 2%, (d) 3%, (e) 4%, (f) 5%, (g) 6% in frequency range of 1780–1680 cm^{-1}. (b) Representative Gaussian fitting of the carbonyl band demonstrating two C=O populations: 'free' carbonyls (1743 cm^{-1}) and the hydrogen-bonded carbonyl groups (1727 cm^{-1}).

interactions of the O–H groups of the GMO and water molecules. In contrast to H_2O, D_2O does not absorb in this region, and by using D_2O in these experiments we were able to follow the effect of CSA solubilization on the O–H stretching mode of the surfactant, without the contribution of the water O–H stretching. As a rule, the stronger the hydrogen bonding between the surfactant O–H groups and the D_2O, the lower the stretching frequency of the O–H group (υ_{OH}). Therefore, by analyzing these bands the O–H groups

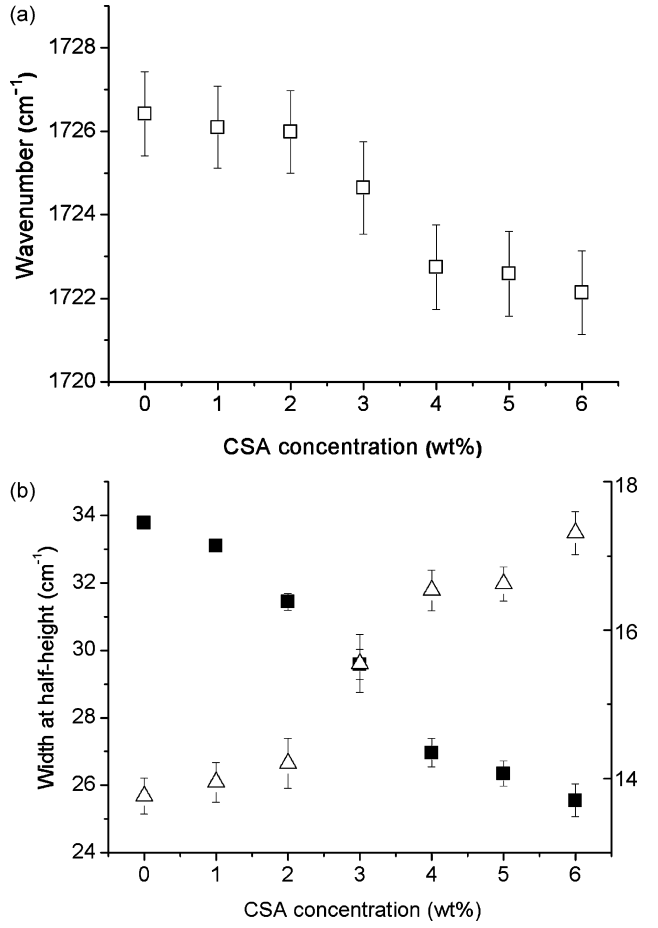

Fig. 8. (a) Frequency (cm^{-1}) as a function of CSA concentration (wt%) of the hydrogen-bonded C=O absorption mode of the surfactant molecules. (b) Width at half-height (cm^{-1}) as a function of CSA concentration (wt%) of the C=O absorption modes of surfactant molecules. (■) Hydrogen-bonded carbonyls (left *y*-axis) (Δ) free carbonyls (right *y*-axis).

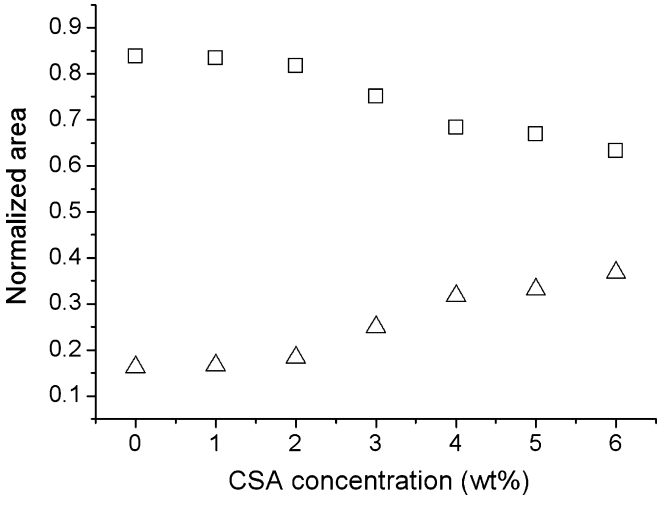

Fig. 9. The normalized peak area ($A_{free}/(A_{free}+A_{bonded})$) and $A_{bonded}/(A_{free}+A_{bonded})$ of the free and hydrogen-bonded carbonyl groups. (□) Hydrogen-bonded carbonyls and (Δ) free carbonyls.

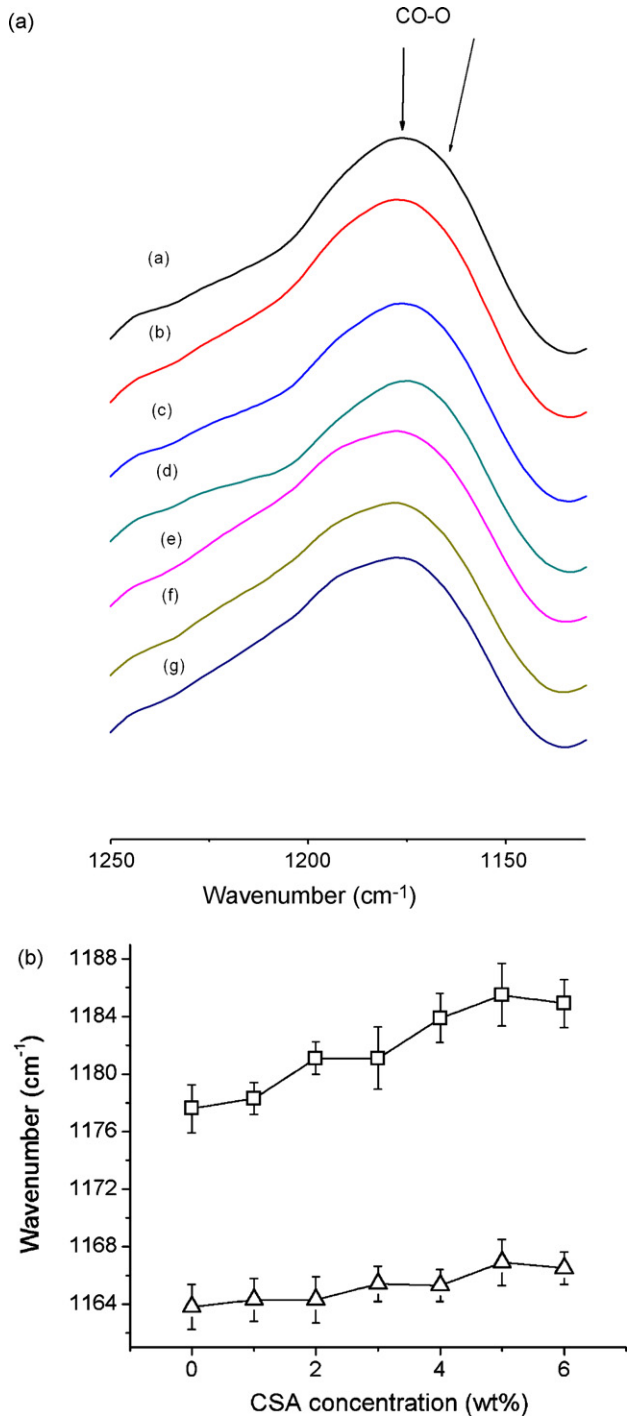

Fig. 10. (a) ATR-FTIR spectra of the H_{II} mesophases of GMO/PC/tricaprylin/water/CSA systems with CSA concentrations of (a) 0%, (b) 1%, (c) 2%, (d) 3%, (e) 4%, (f) 5%, (g) 6% in frequency range of 1100–1300 cm^{-1} showing two absorption maxima of the CO–O groups. (b) Frequency (cm^{-1}) as a function of CSA concentration (wt%) of CO–O absorption modes of the surfactant molecules.

of GMO and interfacial D_2O interactions can be probed. Starting from a concentration of 4 wt% CSA, the position of υ_{OH} was shifted towards higher frequencies, suggesting a weakening of the hydrogen bonds between the between the surfactant O–H groups and the D_2O (Fig. 11). Hence, some degree of dehydration of the GMO hydroxyls occurred as a result of the drug solubilization, indicating a weak interaction of the drug with the O–H groups in the interfacial water region. Bearing in mind the high lipophilicity of the peptide this is an unexpected result. However, Fahr and Seelig (2001) reported that despite the high lipophilicity of the peptide, it exhibits remarkably high exchange rates between liposomes. These results assume some structural transformations in the internal structure of the peptide allowing it to interact with hydrophilic moieties of the surfactants and water. The present findings can also explain the macroscopic properties of these liquid crystals as a result of CSA solubilization (Libster et al., 2007). The described interactions of the peptide with the H_{II} mesophases are expected to weaken the interface and hence influence the rheological behavior of the structures. We demonstrated that the presence of the peptide led to a dramatic decrease in the relaxation times (τ_{max}), the elasticity and the complex viscosity resulting in more fluid-like behavior (Libster et al., 2007). The decrease in τ_{max} and the elasticity of the systems are probably a result of the intercalation of CSA to the interfacial region and its interaction with the carbonyl groups of the surfactants and weakening of the hydrogen bonds between the between the surfactant O–H groups and water.

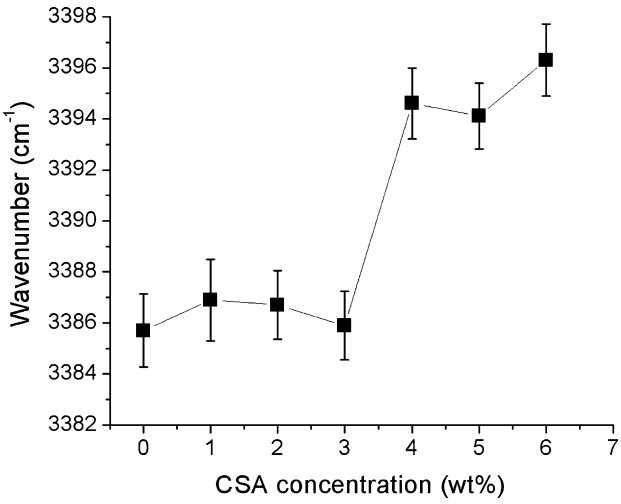

Fig. 11. Frequency (cm^{-1}) as a function of CSA concentration (wt%) of the O–H absorption modes of the surfactant molecules.

3.3. The conformation of CSA in the H_{II} mesophases

In light of the previous unexpected findings we probed the peptide conformation in the H_{II} mesophases. The Amide I' region (1600–1700 cm^{-1}) is widely used for analysis of protein secondary structure and conformational changes. This band appears to be mainly the C=O stretching vibration (~80%) of the amide groups coupled with in-plane NH bending (~20%). Each type of secondary structure results in a unique C=O stretching frequency due to different molecular geometry and hydrogen-bonding strength. Therefore, each band of the Amide I' region is dictated by the backbone conformation and hydrogen-bonding pattern (Vass et al., 2003; Zhang and Yan, 2005). The measured Amide I' band of CSA was featureless (Fig. 12a) since it consisted of overlapping individual bands of secondary structure components. The band was resolved by second derivative analysis. This resolution enhancement method is a well-established technique allowing decomposition of the Amide I' contours into the contributing components (Zhang and Yan, 2005). The absorptions appeared between 1625 and 1700 cm^{-1} as shown at representative spectra (Fig. 12b–d). The resolved Amide I' bands of the peptide are shown in Table 2. It has been suggested that bands below 1645 cm^{-1} appear as a result of hydrogen-bonded C=O groups while "free" carbonyls give rise to absorptions above 1660 cm^{-1}. Bands in the

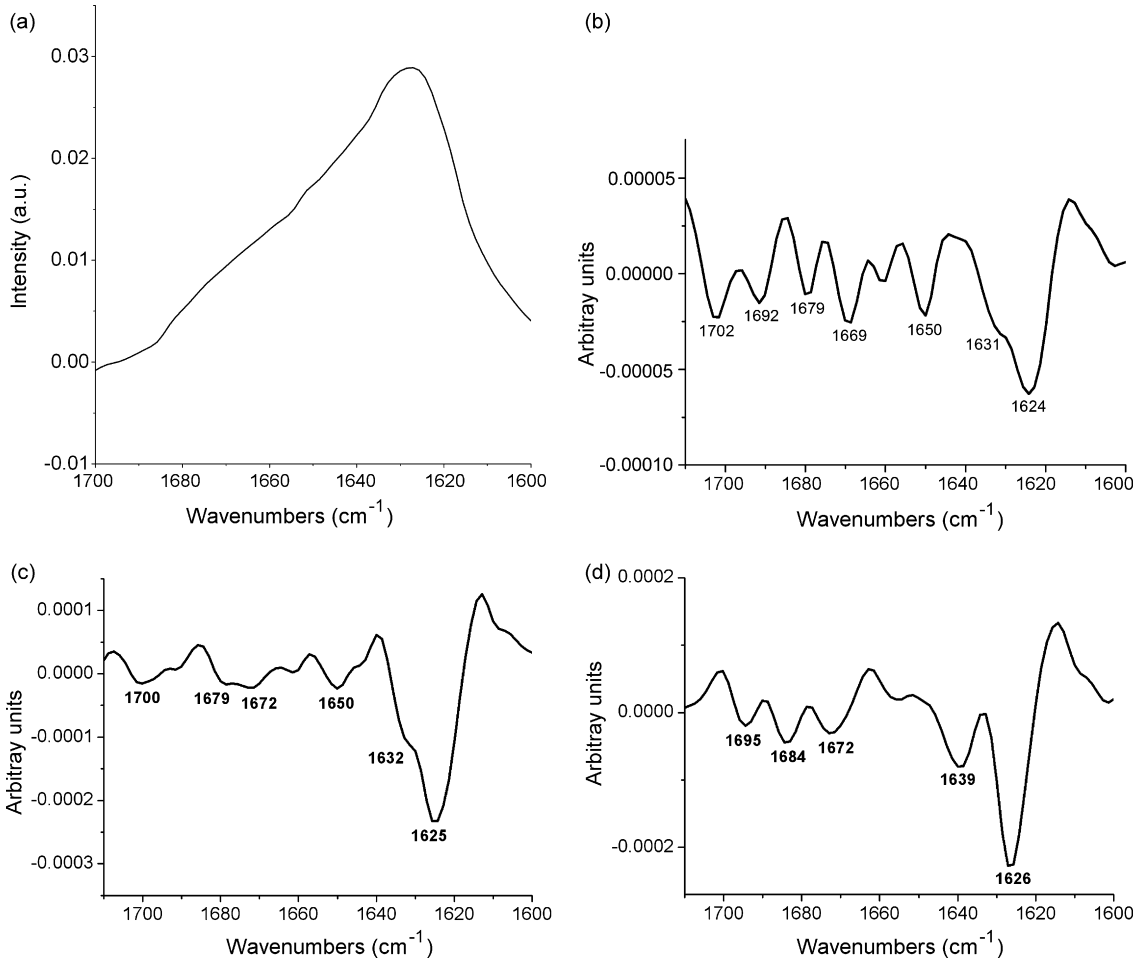

Fig. 12. (a) Amide I' band of GMO/PC/tricaprylin/water/CSA systems with CSA concentration of 4%. (b–d) Representative second derivative FT-IR spectra of CSA incorporated in (b) 2 wt% CSA in H_{II} system, (c) 4 wt% CSA in H_{II} system, (d) 4 wt% CSA in tricaprylin.

1645–1660 range correspond to relatively weak hydrogen-bonded C═O groups that belong to unordered structures. From the spectra it was noticed that the sharpness and intensity of the bands assigned to non-hydrogen-bonded or weak hydrogen-bonded C═O of the higher CSA concentrations (Fig. 12c) decreased compared to the lower content drug samples (Fig. 12b). This indicated a decrease in structural stability of the free and weak hydrogen-bonded carbonyls at high CSA content (4–6 wt%), suggesting the location of the drug in more polar environment at higher peptide concentrations.

Four intramolecularly hydrogen-bonded amide groups were previously detected in the structure of Cyclosporin A by NMR spectroscopy (Altschuh et al., 1994) and FTIR analysis (Shaw et al., 1994; Stevenson et al., 2003; Bodack et al., 2004). Three of the hydrogen bonds stabilize the antiparallel β-sheet structures Val^5NH to $Abu^2C═O$, Abu^2NH to $Val^5C═O$, and Ala^7NH to $MeVal^{11}C═O$. The last hydrogen bond (between Ala^8NH to $MeLeu^6C═O$) stabilizes the γ-loop (Fig. 2).

The representative ATR-FTIR spectra of the peptide solubilized in the H_{II} mesophases are presented in Fig. 12b and c. The following bands were detected and assigned according to the previously published data (Stevenson et al., 2003). The high intensity band at 1624–1625 cm^{-1} was interpreted as an anti-parallel β-sheet with two hydrogen bonds: Ala^7NH to $MeVal^{11}C═O$ and $D\text{-}Ala^8NH$ to $MeLeu^6C═O$. The 1632 cm^{-1} shoulder in midsize cyclic peptides can be assigned to the H-bonded γ-turn, which was probably formed with $D\text{-}Ala^8NH$ to $MeLeu^6C═O$ hydrogen bonding in the present case. The inverse γ-loop consisting of at $D\text{-}Ala^8$, $MeLeu^9$ and $MeLeu^{10}$ was assigned to the 1650 cm^{-1} band. The band at 1669–1672 cm^{-1} was attributed to Type II β-turn located at Sar^3 and $MeLeu^4$. A band at 1679–1681 cm^{-1} reflected the intramolecular hydrogen bond between the β-OH (of CSA) on $MeBmt^1$ and the $MeBmt^1C═O$. The presence of this band also in spectra of CSA embedded within the LLC indicates that the β-OH did not fully bind to the mesophase components. The bands at 1690–1700 cm^{-1} probably reflected the "free", non-hydrogen-bonded C═O of the β-sheet. The ATR-FTIR spectra of CSA solubilized within the liquid crystals was compared to the drug samples within tricaprylin as a reference system (Fig. 12d). Tricaprylin is one of the components of our systems and is a lipophilic oil, which is expected to interact with CSA mainly through hydrophobic interactions. The most obvious difference in the behavior observed when CSA was in tricaprylin is the appearance of a 1639 cm^{-1} peak (Fig. 12d). The bands at 1640 ± 5 in small and cyclic peptides are generally associated with amide groups of H-bonded β-turns (Vass et al., 2003). The 1639 cm^{-1} peak can be interpreted as the Type II β-turn stabilized by two hydrogen bonds – Abu^2NH to $Val^5C═O$ and Val^5NH to $Abu^2C═O$. This means that the Type II β-turn stayed intact in the apolar solvent, which is consistent with the conformation of the peptide in hydrophobic solvents (Stevenson et al., 2003). The lack of this peak in spectra of CSA solubilized within the liquid crystalline structures indicates that these two pairs of hydrogen bonds were disrupted, suggesting partial location of CSA in polar or amphiphilic environment. The implication of this result is that these pairs of the internal hydrogen bonds were broken in order to interact with the surfactants.

Indeed, as was shown above, such interactions were monitored by the changes in the carbonyl and hydroxyl bands of the surfactants as a result of CSA solubilization. Hence, the partial disruption of the internal hydrogen bonds probably allowed rotation of the peptide amide groups outwards. This structural alteration would allow hydrogen bonding between the carbonyls of the surfactants (electron donors) and hydrogens of the peptide. This kind of interaction enabled CSA to be intercalated within the interface region of the H_{II} mesophases. It was demonstrated by several investigators that disruption of the internal hydrogen bonds depicts the active conformation of the drug when rotation of four amide groups outwards to bond with the solvent or the active site takes place (Weber et al., 1991; Wuthrich et al., 1991). The active conformation, explored from receptor binding studies with cyclophilin, was characterized by complete disruption of the secondary structure, including the β-sheet and β-turn conformations.

Another important difference between the spectra of CSA solubilized in the liquid crystals and tricaprylin is the lack of the band at 1648 cm^{-1} and its 1632 cm^{-1} shoulder, which were assigned as an inverse γ-loop consisting of D-Ala[8], MeLeu[9] and MeLeu[10] and a γ-turn formed with D-Ala[8]NH to MeLeu[6]C=O hydrogen-bonding, respectively. The lack of the 1648 cm^{-1} band indicates a loss of the γ-loop structure in hydrophobic tricaprylin. This can be attributed to the hydrogen bond between D-Ala[8]NH and MeLeu[6]C=O, which bifurcates to include the D-Ala[8]C=O. Bonding of the amide proton between two carbonyls results in a twist in the backbone conformation at D-Ala[8]. This, in turn, changes the orientation of the MeLeu[10] side chain, and destabilizes the γ-loop. Similar results were demonstrated by Stevenson et al. (2003) when CSA was dissolved in chloroform and octanol, apolar solvents with no hydrogen bond accepting or donating ability. The loss of the γ-turn was also probably caused by the bifurcation of D-Ala[8]NH. Hence, it seems that the bifurcation of D-Ala[8]NH was prevented in the liquid crystalline mesophases, enabling the D-Ala[8]NH to bond with the surfactants instead of the second peptide backbone carbonyl D-Ala[8]C=O. Fig. 13 visualizes the possible conformations of CSA in tricaprylin, compared to its conformation in the H_{II} mesophase.

From the above FTIR data it could be suggested that the solubilization of CSA into the amphiphilic environment of the liquid crystals caused the peptide to be more hydrophilic by partly disrupting the internal hydrogen bonds and exposing the amide groups to the surfactants Therefore, the peptide became less lipophilic, compared to its initial state. This may supply the explanation of CSA's ability to be partly intercalated in the interface region of the hexagonal structure, as illustrated in Fig. 14. This could also explain high exchange rates between liposomes, which were detected by (Fahr and Seelig, 2001). Interaction with surfactants makes CSA more hydrophilic allowing its transfer through hydrophilic domains of the liposomes.

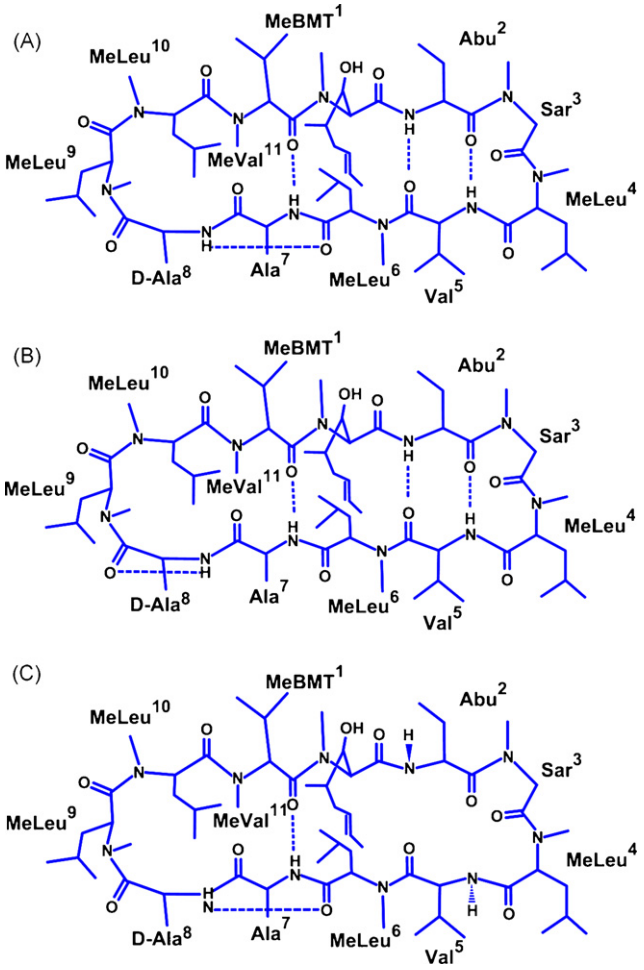

Fig. 13. The possible conformations of CSA in (A and B) tricaprylin, and in the H_{II} mesophase. Note the following differences: (1) γ-loop is destabilized in tricaprylin. This is reflected by two possible alternating conformations, when the hydrogen bond between D-Ala[8]NH and MeLeu[6]C=O (A) bifurcates to include the D-Ala[8]C=O (B). (2) Within the H_{II} mesophase (C) two pairs of hydrogen bonds Abu[2]NH to Val[5]C=O and Val[5]NH to Abu[2]C=O which stabilize Type II β-turn, were disrupted, and γ-loop is stabilized by the hydrogen bond between D-Ala[8]NH and MeLeu[6]C=O.

3.4. Conclusions

As expected, ATR-FTIR spectroscopy proved to be an effective experimental methodology to characterize the detailed structural properties of mixed surfactant H_{II} mesophases at the molecular level. This approach was also very useful to comprehend the influence of the peptide drug CSA on the mesophase structures and to follow the conformational changes of the guest peptide when incorporated within these mesophase carriers. It was found that incorporation of PC to the mesophases had pronounced effect on the GMO–water interface region within the resulting structures. From the results obtained in the present study it seems that the incorporated PC led to competition for water binding between the hydroxyl groups of GMO and the phosphate groups of the PC. Hence, the process detected here eventually leads to dehydration of the hydroxyls in favor of phospholipid hydration within the newly made mesophase structure. Additional evidence was also obtained indicating that the incorporated PC interacts relatively strongly with the β–C–OH groups within the mesophase. In addition, competition between the PC and TAG molecules for solvation of the GMO tails took place, leading to "salting out" of the triglyceride molecules in favor of the PC–GMO interactions.

The solubilization of highly hydrophobic peptide CSA to the H_{II} mesophases revealed unexpected modifications in the interfacial behavior of the loaded mesophases, while the conformation acyl tails of the surfactants were less influenced. The results of the current study indicated that embedding of CSA in the mesophase induced a significant increase in the strength of hydrogen bonding with hydrogen-bonded carbonyls, indicating interaction of the peptide with the C=O groups of the surfactants. These kinds of interactions were mainly reflected in the more restricted conformation of the intramolecularly bounded carbonyls and increased degree of rotation of the free carbonyls as a function of CSA incorporation in the mesophase. The incorporated peptide seemed to cause a partial replacement of the intramolecular hydrogen bonds of the mesophase carbonyl groups with intermolecular hydrogen bonds

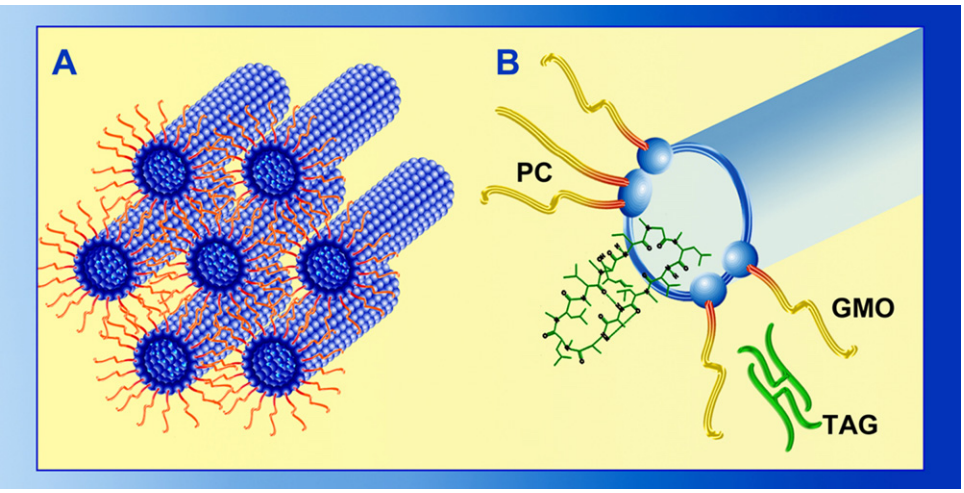

Fig. 14. (a) Schematic presentation of the supramolecular organization of H_{II} mesophase, showing the cylinders packing. (b) Schematic illustration focused on one cylinder of the mixed surfactants (GMO and PC) hexagonal system organization and the localization of CSA within the structure. Note that GMO and PC polar moieties are hydrated, while TAG is located between the lipophilic chains of the surfactants. The peptide is partly intercalated into the interface region of the mesophase, as a result of the disruption of two pairs of internal hydrogen bonds that are available to interact with water or the surfactants heads. It should be noted that the molecular ratio between all the components should not be determined from the image.

of these carbonyl groups with the guest peptide CSA. These conclusions were reinforced by probing the CO–O bond (ester) stretching mode of the surfactants. Analysis of this band revealed a deviation from the dihedral angle of 180° in this segment and implied a more ordered state of CO–O bond, adopting a planar all-trans conformation.

It seems that the observed interfacial interactions of the guest CSA were enabled by specific conformational changes of this rather rigid cyclic peptide when incorporated within the mesophase structure. Analysis of the Amide I' peak in the FTIR spectra of the peptide (in hydrophobic tricaprylin and embedded within the carriers) demonstrated that two pairs of its internal hydrogen bonds were disrupted when it is incorporated. As a result of this, the original γ-turn structure of the cyclic peptide was destabilized, probably re-arranging into a more open conformation that interacts with the polar or amphiphilic parts of the host structure. The partial disruption of the internal hydrogen bonds of the CSA frame seems to cause a rotation of the involved peptide amide groups outwards, resulting in more efficient intermolecular hydrogen bonds and leading to a better solubilization of the CSA within the interface region of the H_{II} mesophases. Obviously, this conformational change significantly increases the hydrophilic properties of CSA, making it more susceptible to a wide range of solubilization and transfer processes. As such, the structural findings reported here provide not only a better insight into the structure and conformation of CSA in different environments, but also a better understanding of various transfer processes of this important peptide drug using carriers based on amphiphilic molecules.

References

Aliabadi, H.M., Elhasi, S., Mahmud, A., Gulamhusein, R., Mahdipoor, P., Lavasanifar, A., 2007. Encapsulation of hydrophobic drugs in polymeric micelles through co-solvent evaporation: the effect of solvent composition on micellar properties and drug loading. Int. J. Pharm. 329, 158–165.

Altschuh, D., Braun, W., Kallen, J., Mikol, V., Spitzfaden, C., Thierry, J.-C., Vix, O., Walkinshaw, M.D., Wüthrich, K., 1994. Conformational polymorphism of cyclosporin A. Structure 2, 963–972.

Amar-Yuli, I., Garti, N., 2005. Transitions induced by solubilized fat into reverse hexagonal mesophases. Colloid Surf. B 43, 72–82.

Amar-Yuli, I., Wachtel, E., Ben Shoshan, E., Danino, D., Aserin, A., Garti, N., 2007a. Hexosome and hexagonal phases mediated by hydration and polymeric stabilizer. Langmuir 23, 3637–3645.

Amar-Yuli, I., Wachtel, E., Shalev, D.E., Aserin, A., Garti, N., 2008. Low viscosity reversed hexagonal mesophases induced by hydrophilic additives. J. Phys. Chem. B 112, 3971–3982.

Amar-Yuli, I., Wachtel, E., Shalev, D.E., Moshe, H., Aserin, A., Garti, N., 2007b. Thermally induced fluid reversed hexagonal (H_{II}) mesophase. J. Phys. Chem. B 111, 13544–13553.

Barth, A., 2007. Infrared spectroscopy of proteins. Biochim. Biophys. Acta 1767, 1073–1101.

Bender, F., Chilcott, T.C., Coster, H.G.L., Hibbert, D.B., Gooding, J.J., 2007. Characterisation of mesoporous polymer films deposited using lyotropic liquid crystal templating. Electrochim. Acta 52, 2640–2648.

Bodack, L.A., Freedman, T.B., Chowdhry, B.Z., Nafie, L.A., 2004. Solution conformations of cyclosporins and magnesium-cyclosporin complexes determined by vibrational circular dichroism. Biopolymers 73, 163–177.

Boyd, B.J., Khoo, S.-M., Whittaker, D.V., Davey, G., Porter, C.J.H., 2007. A lipid-based liquid crystalline matrix that provides sustained release and enhanced oral bioavailability for a model poorly water soluble drug in rats. Int. J. Pharm. 340, 52–60.

Boyd, B.J., Whittaker, D.V., Khoo, S.-M., Davey, G., 2006. Lyotropic liquid crystalline phases formed from glycerate surfactants as sustained release drug delivery systems. Int. J. Pharm. 309, 218–226.

Clogston, J., Caffrey, M., 2005. Controlling release from the lipidic cubic phase. Amino acids, peptides, proteins and nucleic acids. J. Control. Release 107, 97–111.

Dan-Dan, Z., Mao, W.X., Wen-Jia, Z., Jin, Z., Hu, L.L., 2008. Preparation of ordered mesoporous nickel oxide film electrodes via lyotropic liquid crystal templated electrodeposition route. Electrochim. Acta 53, 2699–2705.

Dong, A., Huang, P., Caughey, W.S., 1990. Protein secondary structures in water from second-derivative Amide I infrared spectra. Biochemistry 29, 3303–3308.

Drummond, C.J., Fong, C., 1999. Surfactant self-assembly objects as novel drug delivery vehicles. Curr. Opin. Colloid Interf. Sci. 4, 449–456.

Efrat, R., Aserin, A., Garti, N., 2008. On structural transitions in a discontinuous micellar cubic phase loaded with sodium diclofenac. J. Colloid Interf. Sci. 321, 166–176.

Fahr, A., Hoogevest, P.V., May, S., Bergstrand, N., Leigh, M.L.S., 2005. Transfer of lipophilic drugs between liposomal membranes and biological interfaces: consequences for drug delivery. Eur. J. Pharm. Sci. 26, 251–265.

Fahr, A., Seelig, J., 2001. Liposomal formulations of Cyclosporin A: a biophysical approach to pharmacokinetics and pharmacodynamics. Crit. Rev. Ther. Drug Carrier Syst. 18, 141–172.

Farkas, E., Kiss, D., Zelkó, R., 2007. Study on the release of chlorhexidine base and salts from different liquid crystalline structures. Int. J. Pharm. 340, 71–75.

Fournier, I., Barwicz, J., Auger, M., Tancréde, P., 2008. The chain conformational order of ergosterol- or cholesterol-containing DPPC bilayers as modulated by Amphotericin B: a FTIR study. Chem. Phys. Lipids 151, 41–50.

Gabizon, A., Shmeeda, H., Barenholz, Y., 2003. Pharmacokinetics of pegylated liposomal doxorubicin – review of animal and human studies. Clin. Pharmacokinet. 42, 419–436.

Getie, M., Wohlrab, J., Neubert, R.H.H., 2005. Dermal delivery of desmopressin acetate using colloidal carrier systems. J. Pharm. Pharmacol. 57, 423–427.

Guillén, M., Cabo, D.N., 1997. Infrared spectroscopy in the study of edible oils. J. Sci. Food Agric. 75, 1–11.

Gursoy, R.N., Benita, S., 2004. Self-emulsifying drug delivery systems (SEDDS) for improved orFal delivery of lipophilic drugs. Biomed. Pharmacother. 58, 173–182.

Holmgren, A., Lindblom, G., Johansson, L.B.-Å., 1988. Intramolecular hydrogen bonding in a monoglyceride lipid studied by fourier transform infrared spectroscopy. J. Phys. Chem. 92, 5639–5642.
Hübner, W., Blume, A., 1998. Interactions at the lipid–water interface. Chem. Phys. Lipids 96, 99–123.
Hübner, W., Mantsch, H.H., 1991. Orientation of specifically $^{13}C{=}O$ labeled phosphatidylcholine multilayers from polarized attenuated total reflection FT-IR spectroscopy. Biophys. J. 59, 1261–1272.
Hussain, S., Grandy, D.B., Reading, M., Craig, D.Q.M., Craig, 2004. A study of phase separation in peptide-loaded HPMC films using Tzero-modulated temperature DSC, atomic force microscopy, and scanning electron microscopy. J. Pharm. Sci. 93, 1672–1681.
Italia, J.L., Bhardwaj, V., Kumar, M.N.V.R., 2006. Disease, destination, dose and delivery aspects of ciclosporin: the state of the art. Drug Discov. Today 11, 846–854.
Lake, J.A., 1967. An iterative method of slit-correcting small angle X-ray data. Acta Crystallogr. 23, 191–194.
Lambros, M.P., Rahman, Y.E., 2004. Effects of Cyclosporin A on model lipid membranes. Chem. Phys. Lipids 131, 63–69.
Larsson, K., 1989. Cubic lipid–water phases: structures and biomembrane aspects. J. Phys. Chem. 93, 7304–7314.
Legrue, S.J., Friedman, A.W., Kahan, B.D., 1983. Binding of cyclosporine by human lymphocytes and phospholipid-vesicles. J. Immunol. 131, 712–718.
Libster, D., Aserin, A., Wachtel, E., Shoham, G., Garti, N., 2007. An H_{II} liquid crystal-based delivery system for cyclosporin A: physical characterization. J. Colloid Interf. Sci. 308, 514–524.
Libster, D., Ben Ishai, P., Aserin, A., Shoham, G., Garti, N., 2008. From the microscopic to the mesoscopic properties of lyotropic reverse hexagonal liquid crystals. Langmuir 24, 2118–2127.
Liu, H., Wang, Y., Li, S., 2007. Advanced delivery of Cyclosporin A: present state and perspective. Expert Opin. Drug Deliv. 4, 349–358.
Lopes, L.B., Lopes, J.L.C., Oliveira, D.C.R., Thomazini, J.A., Garcia, M.T.J., Fantini, M.C.A., Collett, J.H., Bently, M.V.L.B., 2006a. Liquid crystalline phases of monoolein and water for topical delivery of Cyclosporin A: characterization and study of in vitro and in vivo delivery. Eur. J. Pharm. Biopharm. 63, 146–155.
Lopes, L.B., Ferreira, D.A., De Paula, D., Garcia, M.T.J., Thomazini, J.A., Fantini, M.C.A., Bently, V.L.B., 2006b. Reverse hexagonal phase nanodispersion of monoolein and oleic acid for topical delivery of peptides: in vitro and in vivo skin penetration of cyclosporin A. Pharm. Res. 23, 1332–1342.
Lopes, L.B., Speretta, F.F.F., Bentley, M.V.L.B., 2007. Enhancement of skin penetration of vitamin K using monoolein-based liquid crystalline systems. Eur. J. Pharm. Sci. 32, 209–215.
Mendelsohn, R., Davies, M.A., Schuster, H.F., Xu, Z., Bittman, R., 1991. CD_2 rocking modes as quantitative infrared probes of one-, two-, and three-bond conformational disorder in dipalmitoylphosphatidylcholine and dipalmitoylphosphatidylcholine/cholesterol mixture. Biochemistry 30, 8558–8563.
Misiunas, A., Niaura, G., Talaikytė, Z., Eicher-Lorka, O., Razumas, V., 2005. Infrared and Raman bands of phytantriol as markers of hydrogen bonding and interchain interaction. Spectrochim. Acta Part A 62, 945–957.
Nilsson, A., Holmgren, A., Lindblom, G., 1991. Fourier-transform infrared spectroscopy study of dioleoylphosphatidylcholine and monooleoylglycerol in lamellar and cubic liquid crystals. Biochemistry 30, 2126–2133.
Nilsson, A., Holmgren, A., Lindblom, G., 1994. An FTIR study of the hydration and molecular ordering at phase transitions in the monooleoylglycerol/water system. Chem. Phys. Lipids 71, 119–131.
Qiu, H., Caffrey, M., 2000. The phase diagram of the monoolein/water system: metastability and equilibrium aspects. Biomaterials 21, 223–234.
Razumas, V., Larsson, K., Miezes, Y., Nylander, T., 1996. A cubic monoolein-cytochrome C-water phase: X-ray diffraction, FT-IR, differential scanning calorimetric and electrochemical studies. J. Phys. Chem. 100, 11766–11774.
Sagalowicz, L., Mezzenga, R., Leser, M.E., 2006b. Investigating reversed liquid crystalline mesophases. Curr. Opin. Colloid Interf. Sci. 11, 224–229.
Sagalowicz, L., Leser, M.E., Watzke, H.J., Michel, M., 2006a. Monoglyceride self-assembly structures as delivery vehicles. Trends Food Sci. Technol. 17, 204–214.
Shah, M.H., Paradkar, A., 2005. Cubic liquid crystalline glyceryl monooleate matrices for oral delivery of enzyme. Int. J. Pharm. 294, 161–171.
Shaw, R.A., Mantsch, H.H., Chowdhry, B.Z., 1994. Conformational changes in the cyclic undecapeptide cyclosporin induced by interaction with metal ions. An FTIR study. Int. J. Biol. Macromol. 16, 143–148.
Song, K.-H., Fasano, A., Eddington, N.D., 2008. Effect of the six-mer synthetic peptide (AT1002) fragment of zonula occludens toxin on the intestinal absorption of cyclosporin A. Int. J. Pharm. 351, 8–14.
Stevenson, C.L., Tan, M.M., Lechuga-Ballesteros, D., 2003. Secondary structure of cyclosporine in a spray-dried liquid crystal by FTIR. J. Pharm. Sci. 92, 1832–1843.
Swarnakar, N.K., Jain, V., Dubey, V., Mishra, D., Jain, N.K., 2007. Enhanced oromucosal delivery of progesterone via hexosomes. Pharm. Res. 24, 2223–2230.
Talaikytė, Z., Barauskas, J., Niaura, G., Švedaitė, I., Butkus, E., Razumas, V., Nylander, T., 2004. Interactions of cyclic AMP and its dibutyrylanalogue with a lipid layer in the aqueous mixtures of monoolein preparation and dioleoyl phosphatidylcholine as probed by X-ray diffraction and Raman spectroscopy. J. Biol. Phys. 30, 83–96.
Vass, E., Hollosi, M., Besson, F., Buchet, R., 2003. Vibrational spectroscopic detection of beta- and gamma-turns in synthetic and natural peptides and proteins. Chem. Rev. 103, 1917–1954.
Weber, C., Wider, G., von Freyberg, B., Traber, R., Braun, W., Widmer, H., Wuthrich, K., 1991. The NMR structure of cyclosporin A bound to cyclophilin in aqueous solution. Biochemistry 30, 6563–6574.
Woo, J.S., Piao, M.G., Li, D.X., Ryu, D.-S., Choi, J.Y., Kima, J.-A., Kim, J.H., Jin, S.G., Kim, D.-D., Lyoo, W.S., Yong, C.S., Choi, H.-G., 2007. Development of cyclosporin A-loaded hyaluronic microsphere with enhanced oral bioavailability. Int. J. Pharm. 345, 134–141.
Wuthrich, K., von Freyberg, B., Weber, C., Wider, G., Traver, R., Widmer, H., Braun, W., 1991. Receptor-induced conformation change of the immunosuppressant cyclosporin A. Science 254, 953–954.
Zhang, J., Yan, Y.-B., 2005. Probing conformational changes of proteins by quantitative second-derivative infrared spectroscopy. Anal. Biochem. 340, 89–98.
Zidan, A.S., Sammour, O.A., Hammad, M.A., Megrab, N.A., Habib, M.J., Khan, M.A., 2007. Quality by design: understanding the formulation variables of a Cyclosporine A self-nanoemulsified drug delivery systems by Box–Behnken design and desirability function. Int. J. Pharm. 332, 55–63.
Zijlstra, G.S., Rijkeboer, M., Jan van Drooge, D., Sutter, M., Jiskoot, W., van de Weert, M., Hinrichs, W.L., Frijlink, H.W., 2007. Characterization of a cyclosporine solid dispersion for inhalation. AAPS J. 9, E190–E199.